

DIFFRACTION OF LIGHT

PACS numbers: 42.79.Jq; 42.30.–d
DOI: 10.1070/QE2015v045n02ABEH015385

Spatial and spectral image distortions caused by diffraction of an ordinary polarised light beam by an ultrasonic wave

A.S. Machihin, V.E. Pozhar

Abstract. **We consider the problem of determining the spatial and spectral image distortions arising from anisotropic diffraction by ultrasonic waves in crystals with ordinary polarised light (o → e). By neglecting the small-birefringence approximation, we obtain analytical solutions that describe the dependence of the diffraction angles and wave mismatch on the acousto-optic (AO) interaction geometry and crystal parameters. The formulas derived allow one to calculate and analyse the magnitude of diffraction-induced spatial and spectral image distortions and to identify the main types of distortions: chromatic compression and trapezoidal deformation. A comparison of the values of these distortions in the diffraction of ordinary and extraordinary polarised light shows that they are almost equal in magnitude and opposite in signs, so that consistent diffraction (o → e → o or e → o → e) in two identical AO cells rotated through 180° in the plane of diffraction can compensate for these distortions.**

Keywords: *acousto-optic filter, distortions, acousto-optic diffraction.*

1. Introduction

Instruments for spectral polarisation analysis based on electronically tunable acousto-optic (AO) filters are widely used in various fields of science and technology: microscopy [1], remote sensing [2, 3], endoscopy [1, 4], tomography [5], digital holography [6], astronomy [7] and photoluminescent diagnostics [8]. High spatial and spectral resolution, possibility of modulation and transfer function synthesis and absence of moving elements distinguish them from the devices built on other physical principles. At the same time, fast arbitrary spectral tuning allows one to design spectral adaptive systems on their basis [9].

Despite the fact that the AO filtering of images has long been successfully employed in many applications, it cannot be used due to insufficient quality of images: Chromatic shift of an image complicates the construction of spectra at discrete points [10] and makes it impossible to perform operations on spectral images without additional procedures for their mutual binding [11].

A.S. Machihin, V.E. Pozhar Scientific and Technological Center of Unique Instrumentation, Russian Academy of Sciences, ul. Butlerova 15, 117342 Moscow, Russia; e-mail: aalexanderr@mail.ru, v_pozhar@rambler.ru

Received 18 January 2014; revision received 21 April 2014
Kvantovaya Elektronika **45** (2) 161–165 (2015)
Translated by I.A. Ulitkin

As a result of AO diffraction, spectral and spatial distortions in some cases may reach several percent of the field of view [12, 13]. They are, in principle, can be corrected by post-processing using the data of AO filter pre-calibration [14]. In this case, however, (i) residual distortions, whose value depends essentially on the calibration accuracy, are preserved, and (ii) this approach cannot be always implemented, especially in real time when accurate calibration is difficult and correction time is very limited.

Another approach is to develop a method of hardware distortion correction based on the material selection and configuration of the AO cell, optimal from the point of view of image transmission. Previously it has been shown experimentally and theoretically that the image distortion resulting from the AO interaction can be compensated for by sequential filtration in two identical AO cells rotated through 180° in the polar plane [15]. The systematic nature of distortions and their spectral dependence have been first considered in [16] in the small-birefringence approximation: $\Delta n/n_o = \xi_0 - 1 \ll 1$. Here, $\xi_0 = \xi(0)$; $\xi(\theta_1) = n_e/(n_o^2\cos^2\theta_1 + n_e^2\sin^2\theta_1)^{1/2}$; θ_1 is the angle between the direction of propagation of light in the crystal and the plane perpendicular to its optical axis; $\Delta n = n_e - n_o$; and n_o and n_e are the refractive indices of the crystal material for ordinary and extraordinary polarised waves). In our papers [13, 17], we have calculated these distortions in the general form, but only for the case of AO diffraction of extraordinary polarised light (e → o). For the case of ordinary polarised light diffraction (o → e) the exact analytical solution has not been found, and known only are the estimates of the magnitudes of spatial and spectral distortions in the polar and azimuth planes and in the small-birefringence approximation ($\Delta n/n_o \ll 1$) [16]. For AO crystals used in practice this parameter is not always quite small: $\Delta n/n_o = 0.07$ for TeO_2 (λ = 0.6 μm), –0.1 for $CaCO_3$ (λ = 0.6 μm) and 0.34 for Hg_2Cl_2 (λ = 2 μm), and therefore this approximation does not allow for precise aberration calculation, in particular in assessing the degree of distortion compensation in a 'double-crystal' scheme.

In this paper, the problem of calculating spatial and spectral image distortions caused by AO diffraction o → e is treated in a general case, i.e., not separately in planes *xz* and *xy*, but with allowance for the cross terms in the expansion. The analytical solution is obtained in a significantly weaker (than $\Delta n/n_o \ll 1$) approximation, which assumes the value of ξ to be constant in a small range of angles between the incident (θ_1) and diffracted (ψ_1) light waves: $\xi(\psi_1) \approx \xi(\theta_1)$. In practice, this angular range is 1°–3°. As will be shown below, this assumption for all known uniaxial AO crystals is always satisfied with very high accuracy (better than 15′) in the whole range of θ_1 variation.

2. Basic relations

To solve this problem, it is necessary to relate the arising geometric image distortions to AO cell parameters and AO interaction geometry. An image transferred by a weakly divergent light beam is described by the angular intensity distribution $I(\theta_1, \theta_2)$, where θ_i is an angle determining the propagation direction of a partial wave. The image transformation is described by the dependences $\psi_j(\theta_i)$, which compare the direction of the diffracted wave (ψ_j) with each incident wave (θ_i). Here, the indices i and j take the values 1 and 2 for the polar plane (xz) and for the azimuth plane of the AO interaction, respectively.

To determine these dependences, we consider diffraction of a weakly divergent o-polarised light beam by an acoustic wave in a uniaxial crystal (Fig. 1). The phase-matching condition relating the wave vectors of an incident ($\boldsymbol{k}_\mathrm{i}$) and a diffracted ($\boldsymbol{k}_\mathrm{d}$) light waves to the wave vector of an acoustic wave $\boldsymbol{q}$ has the form $\boldsymbol{k}_\mathrm{d} = \boldsymbol{k}_\mathrm{i} - \boldsymbol{q}$ for the diffraction process accompanied by frequency down-conversion. By passing for clarity to dimensionless quantities as in [17], we can write this equation in the projections on the x, y and z axes:

$$\cos\theta_1\cos\theta_2 - \eta\cos\gamma_1\cos\gamma_2 - \xi(\psi_1)\cos\psi_1\cos\psi_2 = \chi\cos\varphi_1\cos\varphi_2, \quad (1a)$$

$$\cos\theta_1\sin\theta_2 - \eta\cos\gamma_1\sin\gamma_2 - \xi(\psi_1)\cos\psi_1\sin\psi_2 = \chi\cos\varphi_1\sin\varphi_2, \quad (1b)$$

$$\sin\theta_1 - \eta\sin\gamma_1 - \xi(\psi_1)\sin\psi_1 = \chi\sin\varphi_1, \quad (1c)$$

where $\eta = q/(kn_\mathrm{o}) = \lambda/(\Lambda n_\mathrm{o})$ is the dimensionless spectral parameter that determines the ratio of the light wavelength (λ) and sound (Λ); $\chi = \Delta k/(kn_\mathrm{o})$ is the normalised (dimensionless) mismatch; and Δk, φ_1, φ_2 are the length and angles of orientation of the wave mismatch, $\Delta\boldsymbol{k} \equiv \boldsymbol{k}_\mathrm{i} - \boldsymbol{k}_\mathrm{d} - \boldsymbol{q}$.

By using specified values of the angles that determine the propagation direction of light (θ_1, θ_2) and sound (γ_1, γ_2), equations (1) allow one to determine the direction of wave propagation after diffraction (ψ_1, ψ_2) and the magnitude of the wave mismatch χ for any sound wavelength Λ and for each wavelength of ordinary polarised light λ. It should be noted that a beam of diffracted light waves corresponds to each incident plane light wave (this follows from the boundedness of the interaction region). With this in mind, the direction of diffraction is considered to be one in which a wave propagates, which has a minimal wave mismatch Δk and corresponds to a maximum angular intensity of the diffracted wave. Thus, one diffracted wave is compared with each incident wave. The vector orientation of the wave mismatch $\boldsymbol{\Delta k}$ is chosen by using the same principles as in [17]: $\varphi_1 = \theta_1$, $\varphi_2 = \theta_2$. Given this, one can represent the value of ψ_i and χ as a function of the given angles γ_i and θ_i and the spectral parameter η.

Unlike the case of AO diffraction of an extraordinary polarised beam, the exact analytical solution of the system of equations (1) is difficult to obtain, because it is reduced to a polynomial equation of the 6th degree. However, an approximate solution can be found by assuming that in a small range of angles from θ_1 to ψ_1, birefringence is approximately constant, so that $\xi(\psi_1) \approx \xi(\theta_1)$. The exact ratio of these values is given by

$$\frac{\xi(\psi_1)}{\xi(\theta_1)} = \sqrt{\frac{1 + (\xi_0^2 - 1)\sin^2\psi_1}{1 + (\xi_0^2 - 1)\sin^2\theta_1}} = \sqrt{1 + (\xi_0^2 - 1)\sin(\psi_1 - \theta_1)\frac{\sin(\psi_1 + \theta_1)}{1 + (\xi_0^2 - 1)\sin^2\theta_1}}\,. \quad (2)$$

Its difference from unity is determined by the second term under the square root, which contains the product of two small quantities: the birefringence parameter, $\xi_0^2 - 1 \approx 2\Delta n/n_\mathrm{o}$, and the deflection angle of the diffracted wave, $|\psi_1 - \theta_1| \sim 10^{-2}$. Figure 2 shows the dependence of $\xi(\psi_1)/\xi(\theta_1) - 1$ on the angle θ_1, calculated by formula (2) in the case of the wide-angle [18] AO interaction geometry in a TeO_2 crystal used to transmit the images (for this geometry the condition $\tan\psi_1 = \xi_0^{-2}\tan\theta_1$ is satisfied). Hereafter, all of the examples are given for diffraction in the (110) plane of the TeO_2 crystal. One can see that for the filters based on this crystal, $|\xi(\psi_1)/\xi(\theta_1) - 1| \leqslant 2\times10^{-3}$ at any angles θ_1 of light propagation. In this approximation the error of analytical calculation of ψ_1 from (1) does not exceed 15′, while the angular phase-matching width is 2°.

Approximation $\xi(\alpha) = \mathrm{const}$ ($\psi_1 \leqslant \alpha \leqslant \theta_1$) allows one to obtain from equations (1) the formula:

$$\chi \approx 1 - \eta B - \sqrt{\eta^2(B^2 - 1) + \xi^2(\theta_1)}\,, \quad (3a)$$

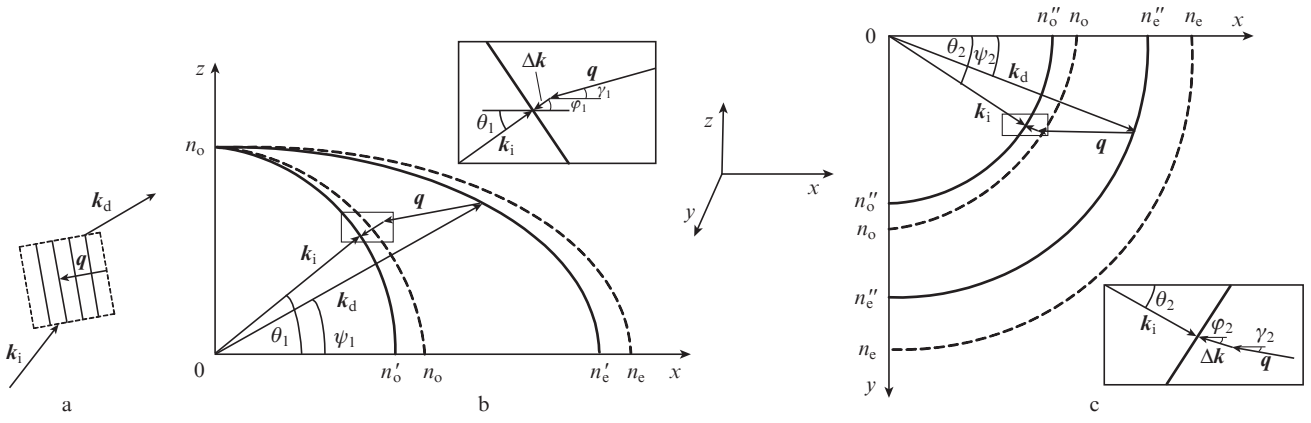

Figure 1. (a) AO interaction region and wave vector diagrams in the (b) polar and (c) azimuth planes in the case of diffraction of the o-polarised light wave ($n_\mathrm{o}' = n_\mathrm{o}\cos\theta_2$, $n_\mathrm{o}'' = n_\mathrm{o}\cos\theta_1$, $n_\mathrm{e}' = n_\mathrm{e}\cos\psi_2$, $n_\mathrm{e}'' = n_\mathrm{e}\cos\psi_1$).

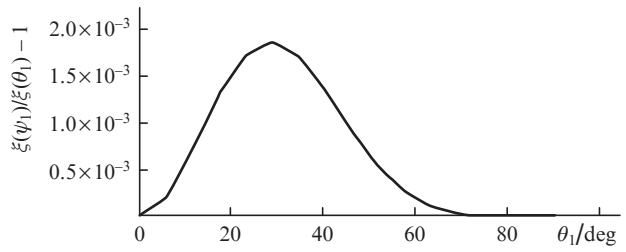

Figure 2. Dependence of $\xi(\psi_1)/\xi(\theta_1) - 1$ on the propagation angle θ_1 in the case of the wide-angle AO interaction geometry in a TeO_2 crystal (λ = 633 nm).

where $B = \cos(\theta_1 - \gamma_1) - \cos\theta_1\cos\gamma_1[1 - \cos(\theta_2 - \gamma_2)]$. Angles ψ_1 and ψ_2 are expressed through χ:

$$\psi_1 \approx \arcsin\left[\frac{(1-\chi)\sin\theta_1 - \sin\gamma_1}{\xi(\theta_1)}\right], \tag{3b}$$

$$\psi_2 \approx \arctan\left[\frac{(1-\chi)\sin\theta_1\sin\theta_2 + \eta\cos\gamma_1\sin\gamma_2}{(1-\chi)\cos\theta_1\cos\theta_2 + \eta\cos\gamma_1\cos\gamma_2}\right]. \tag{3c}$$

Thus, all the characteristics of the diffracted beam (χ, ψ_1, ψ_2) are given in the form of functions of the characteristics of the interacting waves θ_1, θ_2, γ_1, γ_2 and η.

Formulas (3) have a meaning similar to that of the expressions obtained in [17] for diffraction of an e-polarised incident wave. They describe AO diffraction for an arbitrary value of ξ within the entire field of view, and not only in two directions: along the optical axis and perpendicular to it. Angles ψ_1, ψ_2 determine the direction of the diffracted wave, and the dimensionless mismatch χ characterises the diffraction coefficient.

The maximum diffraction coefficient corresponds to the exact matching conditions ($\chi = 0$). For a given direction of incidence of a light wave (θ_1, θ_2), one can find an appropriate direction of diffraction (ψ_{1s}, ψ_{2s}), which will be denoted below by index s (matching). To this end, we find from equation (3a) the spectral parameter $\eta_s(\theta_1, \theta_2)$ corresponding to the exact matching condition($\chi = 0$):

$$\eta_s = B - \sqrt{B^2 + \xi^2(\theta_1) - 1}\,. \tag{4}$$

Substituting this expression into formulas (3b) and (3c) gives the dependences $\psi_{1s}(\theta_1, \theta_2)$ and $\psi_{2s}(\theta_1, \theta_2)$ for given γ_1, γ_2, λ and Λ, which are not presented here because of their awkwardness.

3. Spatial and spectral distortions

To analyse the spatial (angular) distortions, we will consider the dependences (3b) and (3c) and determine for each partial incident beam (θ_1, θ_2) the direction of its propagation after diffraction (ψ_1, ψ_2). It is convenient to operate with the relative position of the beam, counting the angles of propagation of the incident light from a 'central' direction (θ_{1s}, θ_{2s}) and of the diffracted light – from its corresponding exact matching direction [$\psi_{is}(\theta_{1s}, \theta_{2s})$]: $\Delta\theta_i = \theta_i - \theta_{is}$, $\Delta\psi_i = \psi_i - \psi_{is}$. Since the angular divergence of the incident and diffracted beams is small (~2°), which is caused by a small angular matching width, we represent the relationship of diffracted beams with incident ones using formulas (3) and (4) in differential form, by expanding it in a Taylor series over small deviation angles ($|\Delta\theta_i| \ll 1$) and using quadratic terms only:

$$\begin{aligned}\Delta\psi_i(\Delta\theta_1, \Delta\theta_2) &= \Delta\theta_i + b_{i1}\Delta\theta_1 + b_{i2}\Delta\theta_2 + c_{i11}\Delta\theta_1^2 + c_{i12}\Delta\theta_1\Delta\theta_2 + c_{i22}\Delta\theta_2^2 \\ &\equiv A_i + A_{i1} + A_{i2} + A_{i11} + A_{i12} + A_{i22}\,. \end{aligned} \tag{5}$$

In this formula, the first term A_i describes an identity transformation of the beam, and others – different types of image distortion. The expansion coefficients have the following physical meaning: b_{ij} describes linear distortions, i.e., relative scaling (b_{11} and b_{22}) and rotation (b_{12} and b_{21}), and c_{ijk} – nonlinear (quadratic) distortions. Chromatic distortions are also described by this formula, because the expansion coefficients depend on the parameter ξ, which has a spectral dependence due to the dispersion of the refractive indices.

To estimate the magnitude of data distortion, we have performed calculations for basic AO interaction geometries used for image filtering. Figure 3 shows the dependence of the angle of incidence of light, θ_{1s}, on the values of monochromatic linear (A_{i1}, A_{i2}) and nonlinear (A_{i11}, A_{i12}, A_{i22}) distor-

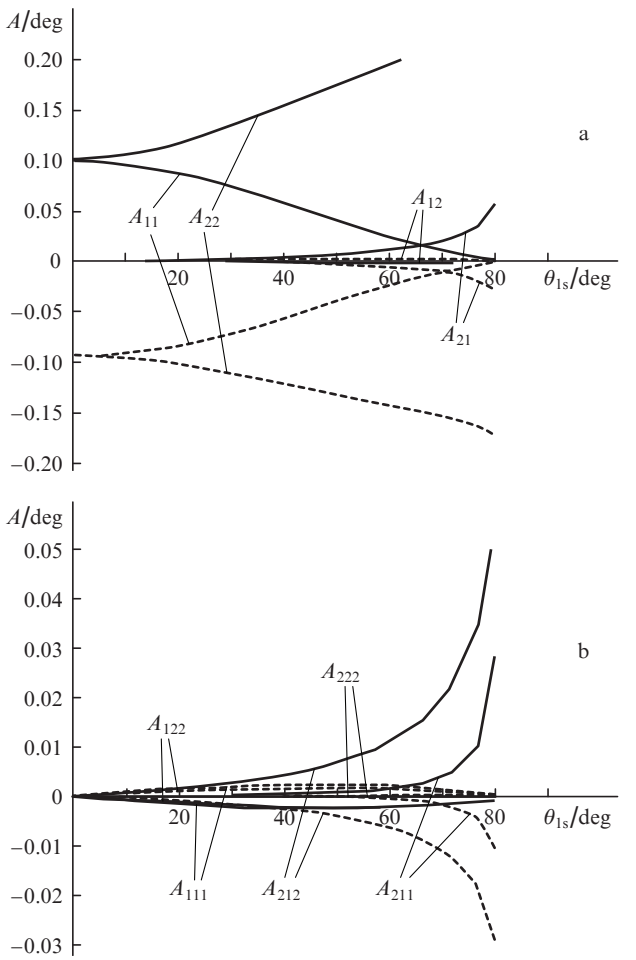

Figure 3. Dependences of the (a) linear and (b) nonlinear distortions introduced into the image by wide-angle AO diffraction (TeO_2, λ = 633 nm, $\delta\theta_1 = \delta\theta_2 = 3°$) on the angle of incidence in the case of diffraction of e-polarised (solid curves) and o-polarised (dashed lines) light. Shown are the maximum distortions that occur at the edge of the field of view.

tions for wide-angle AO diffraction with total angular aperture $\delta\theta_i = 3°$ in paratellurite at a wavelength of $\lambda = 633$ nm. For comparison, Fig. 3 shows similar dependences for the case of diffraction of the e-polarised light, previously calculated in [17].

Analysis of linear distortions for uniaxial crystals shows that image compression dominates in them ($A_{11} < 0$ and $A_{22} < 0$). In the case of collinear AO interaction geometry in the direction perpendicular to the optical axis ($\theta_{1s} = \theta_{2s} = 0$), the compression ratio is the same in both axes ($A_{11} = A_{22}$), and if the beam deviates from this direction, the compression in the azimuth plane becomes dominant ($|A_{22}| > |A_{11}|$). Among nonlinear distortions, dominant is a trapezoidal deformation of an image defined by the term A_{212}. With increasing θ_{1s} this distortion grows and at $\theta_{1s} > 80°$ reaches several percent of the field of view.

Note the special character of collinear diffraction geometry along the x axis ($\theta_{1s} = \theta_{2s} = 0$). Firstly, in this case the first-order image distortions are axially symmetrical, as is clear from the optical symmetry of this direction ([110]). Second, for a given geometry the distortions are minimal: there is only a slight decrease in the image size ($A_{11} = A_{22} > 0$), whereas the values of other coefficients that describe the linear and nonlinear distortions are close to zero.

The spectral dependence of the distortions is determined by the dispersion of the refractive index of the AO cell material, and for example, in the range of 0.4 – 1.0 μm at the same AO diffraction geometry as that in Fig. 3, the distortions amount to about 5% – 10%.

4. Modelling

To illustrate the distortions resulting from the AO interaction, we numerically simulated image transformation in the case of diffraction of the o-polarised light. Figure 4 shows a reference object (square grid) and its calculated images at three wavelengths belonging to different parts of the spectrum: 0.38, 0.55 and 0.78 μm. Calculations were performed for a real wide-angle TeO_2 acousto-optic filter ($\theta_1 = 73.6°$, $\gamma_1 = -8°$) with an aperture $\delta\theta_i = 3°$ in the case of the o-polarised incident light (Fig. 4a) and for a similar AO filter ($\theta_1 = 73.6°$, $\gamma_1 = -7.1°$) in the case of the e-polarised light (Fig. 4b). In these cases, linear distortions dominate, with scaling in the azimuth plane being significantly stronger than in the polar plane ($|A_{22}| > |A_{11}|$) which is consistent with the dependences in Fig. 3.

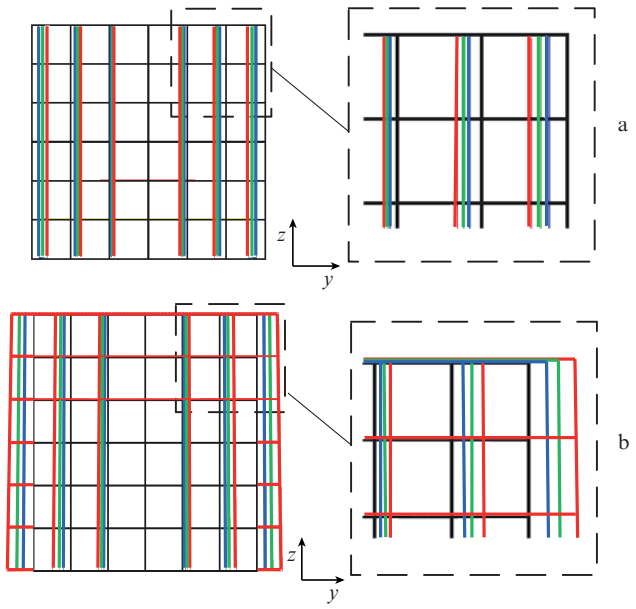

Figure 4. (Colour in online edition) Reference object (black) and its calculated spectral images at $\lambda = 0.38$ μm (blue), 0.55 μm (green) and 0.78 μm (red) in the case of AO diffraction of (a) o-polarised and (b) e-polarised light in a wide-angle TeO_2 filter ($\theta_1 = 73.6°$) with an aperture 3°.

The fact that the images do not coincide with the object indicates the presence of geometric monochromatic aberrations described mainly by the coefficients b_{ij}. Misalignment of spectral images with each other shows the presence of a chromatic aberrations, the value of which at the edge of the field of view reaches 3% – 4% of the image size. The asymmetry of the images, more pronounced on their periphery, illustrates the influence of the cross terms A_{112} and A_{212}.

Analysis of the distortion coefficients (Fig. 3) and the calculated spectral images (Fig. 4) shows that in the wide-angle AO filter for any given angle of incidence θ_{1s}, the type of polarisation has little effect on the magnitude of linear and nonlinear distortions, but determines their sign, i.e. in the case of the e-polarised light diffraction the image is stretched, and in the case of the o-polarised light diffraction, it is compressed. This allows one to substantiate the developed methods of compensation of distortions introduced by the AO cell due to consequent filtration in the two AO cells rotated through 180° in the polar plane [15]. Previously, the theoretical possibility of compensation of spatial and spectral distortions in this scheme has been shown only in the linear approximation [16].

5. Conclusions

In this paper, without using the small-birefringence approximation we have obtained for the first time general analytical solutions (3) describing the dependence of the wave mismatch Δk and diffraction angles ψ_i on the AO interaction geometry (θ_i, γ_i) and the crystal (ξ) and ultrasonic wave (Λ) parameters in the case of diffraction of polarised light. These formulas allow one calculate AO-diffraction-induced spatial and spectral image distortions $\Delta\psi_i$ with an accuracy of ~10% of the angular aperture of the AO cell. Analysis of these distortions has revealed their main types: chromatic asymmetric compression (downscaling) and trapezoidal deformations. Linear distortions in the azimuth plane A_{22} have been found to dominate. We have constructed the dependences of the linear and nonlinear distortions on the angle of incidence of the light, θ_{1s}. The comparison of these distortion coefficients with the corresponding coefficients for the case of diffraction of e-polarised light has shown that their values are fairly close in magnitude but have opposite signs, which, in particular, creates prerequisites for the development of methods for compensating for AO-filtration-induced distortions by using two AO cells located in a certain way.

The results obtained can be used in the analysis and synthesis of optical systems, including AO cell for spectral filtering of images.

Acknowledgements. This work was supported by the Russian Foundation for Basic Research (Grant Nos 14-00-10420_Ir, 13-02-12210 and 15-08-08696).

References

1. Bouhifd M., Whelan M. *Proc. SPIE Int. Soc. Opt. Eng.*, **6628**, 662803 (2007).
2. He Z., Shu R., Wang J. *Proc. SPIE Int. Soc. Opt. Eng.*, **8196**, 819625 (2011).
3. Inoue Y., Penuelas J. *Int. J. Remote Sens.*, **22** (18), 3883 (2001).
4. Pozhar V., Machihin A., Batshev V. *Photonics Lasers Medicine*, **2** (2), 153 (2013).
5. Viskovatykh A.V., Machihin A.S., Pozhar V.E., Pustovoit V.I., Viskovatykh D.A. *Pis'ma Zh. Tekh. Fiz.*, **40**, 33 (2014) [*Tech. Phys. Lett.*, **40**, 157 (2014)].
6. Kim D., Javidi B. *Techn. Dig. Biomedical Topical Meeting* (Washington, DC, OSA, 2004) Paper FH37.
7. Chang L., Yao D., Zhao B., Qiu Y. *Proc. SPIE Int. Soc. Opt. Eng.*, **8910**, 89101Z (2013).
8. Reichmann P., Fried D. *Proc. SPIE Int. Soc. Opt. Eng.*, **8208**, 82080E (2012).
9. Pozhar V.E., Pustovoit V.I. *Radiotekh. Elektron.*, **41** (10), 1272 (1996).
10. Martin M., Wabuyele M., Panjehpour M., et al. *Proc. SPIE Int. Soc. Opt. Eng.*, **5692**, 133 (2005).
11. Gat N. *Proc. SPIE Int. Soc. Opt. Eng.*, **4056**, 50 (2000).
12. Ryu S., You J., Kwak Y., Kim S. *Opt. Express*, **16** (22), 17138 (2008).
13. Machihin A.S., Pozhar V.E. *Kvantovaya Elektron.*, **40** (9), 837 (2010) [*Quantum Electron.*, **40** (9), 837 (2010)].
14. Machihin A.S., Pozhar V.E. *Prib. Tekh. Eksp.*, (6), 92 (2009) [*Instrum. Exp. Tech.*, **52** (6), 847 (2009)].
15. Mazur M.M., Pozhar V.E., Pustovoit V.I., Shorin V.N. *Usp. Sovr. Radioelektron.*, **10**, 19 (2006).
16. Pozhar V., Pustovoit V. *Photonics Optoelectron.*, **4** (2), 67 (1997).
17. Pozhar V., Machihin A. *Appl. Opt.*, **51** (19), 4513 (2012).
18. Chang I.C. *Appl. Phys. Lett.*, **25**, 370 (1974).